Petroleum and Coal

**Article** **Open Access**

# A plausible Seismic Velocity-Effective Stress Transform for Overpressure Prediction: A case study of the Central Swamp Depobelt, Onshore Niger Delta, Nigeria

*J. E. Asedegbega[1], A. I. Opara*[2], M. Omudu[3], and N. N. Onu[2]*

[1] *GCube Integrated Services Limited, Lagos, Nigeria*
[2] *Department of Geology, Federal University of Technology, PMB 1526, Owerri, Nigeria*
[3] *Shell Petroleum Development Company (Nig) Ltd, Port Harcourt, Nigeria*

Received September 6, 2019; Accepted February 4, 2020

**Abstract**

Accurate transform of seismic velocity to formation pressure is vital to safe and cost-effective drilling, especially in frontier basins with little or no offset data. There exist several compaction trend algorithms, most of which are not based on rock physics concepts. Although some progress has been made in the use of rock physics in pore pressure estimation, however a lot of work is still needed in the area of accurate velocity -to-pressure transforms in shale dominated settings. This paper provides a quick and simple model for velocity(Vp) transformation to vertical effective stress (VES) as an input to pore pressure estimation. Shale velocity, density log and measure pore pressure (MPP) data were used to develop a Vp-VES transform for the Onshore Niger Delta Basin. Seismic velocities were picked densely and sparsely respectively (100m and 200m) around wells with MPP data. These interval velocities were applied to the Vp-VES regression from wells to obtain VES cubes from both isotropic and anisotropic Pre-Stack Depth Migration (PSDM) velocity. Seismically-derived Pore Pressure data (PP) were obtained from the differences between overburden stress and VES cubes and further compared with MPP data. The transformed seismic PP approximated the MPP at offset well locations. The resultant velocity profile from the velocity picking proved to be optimal in the transformational process of the seismic PP; therefore, the use of 100m spacing provided adequate spatial resolution. In addition, the inverted anisotropic seismic interval velocities provided a trend that fits with the geology of the study area, far better than the isotropic velocity. The anisotropic PSDM velocity enhanced PP at a pressure gradient greater than 0.7 psi/ft and depth >14000 ft ss with little or no calibration. Therefore, incorporation of anisotropic correction on long offset data and the use of a rock physics constrained Vp-VES transform will ultimately improve seismic PP imaging at deeper intervals.

***Keywords****: Anisotropic correction; isotropic velocity; seismic velocity; vertical effective stress; Pre-stack depth migration; pore pressure.*

## 1. Introduction

In today's oil and gas exploration activities, detailed and accurate knowledge of subsurface pressure regime is very beneficial to seal integrity and hydrocarbon column height estimation as well as in safety optimization and drilling cost reduction. Lack of accurate pre-drill pore pressure profile generally results in cautious drilling and consequently slows down penetration rates, cause excessive bit wear, and increase well cost and risk while drilling [1].

Over the past few decades, seismic velocities in their different vintages change remain to became a major source and, most often, the only input data for large scale pre-drill pore-pressure prediction. This is true, especially for virgin areas and when drilling beyond known depth intervals within the explored areas. The extraction of the target overpressure signature from seismic velocity input is based on the theoretically accepted and practically proven empirical fact that overpressure is measurable from seismic data and therefore, can be extracted and interpreted from the relevant seismic velocity information. Overpressures normally affect the compaction of subsurface rocks, and therefore, changes in the formation velocity can be calibrated to changes in pore pressure, assuming there are no lithological variations. Velocities derived from surface seismic data are, very effective as an indirect means of predicting subsurface pore pressures prior to drilling [2].

Deeper targets in the Onshore Niger Delta are associated with the lack of offset well data, and poor seismic resolution at depths since most seismic surveys in the Niger Delta were shot with a 3.0 km cable offset [2-3]. These deep prospects and plays would, therefore, largely require long, offset wide azimuth seismic data and update on the velocity modelling workflow for optimal prospect evaluation and well design.

The interpretation and extraction of overpressure anomaly from well and seismic velocities reversals are not new. However, the transformation model used in determining an appropriate subsurface rock model for converting velocity to pore pressure accurately still poses some challenges. Hence, a robust model that links rock velocities and stress fields to geology have been proposed in this paper that can be used to transform seismic interval velocity to effective stress as input for accurate shale pressure prediction in the Niger Delta Onshore depositional belts.

### 1.1. Location and geological setting

The study area "Field X'' is located in OML 28 Oil block, about 110 km west of Port Harcourt within the Central Swamp depositional belt of the Niger Delta Basin (Fig. 1). The hydrocarbon reservoir type within the study area is typically sandstone of the shallow marine depositional environment. The first well was discovered in the study area in 1961, with the first oil production executed in 1973. Presently, the total number of wells drilled in the field is 39, with 5 abandoned and 9 producing. Porosity within the field is between 21-28 percent with hydrocarbon interval of 11500-11900 ft for oil, while that of gas ranges between 9200 – 13500 feet. The 3D seismic data was first acquired between July-October 1997 with a short offset and was re-acquired in 1998, with a long cable of about 6.0 km offset. The data set was processed into PSDM velocities in 2007 and 2009, respectively.

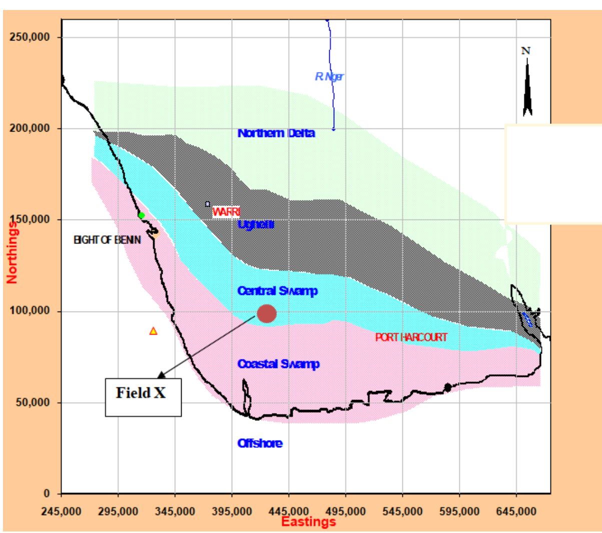


Figure 1. Section map of Nigeria showing the location of the study area in the Niger Delta Basin [13]

The Niger Delta Basin is situated within the Gulf of Guinea and is one of the most prolific hydrocarbon bearing basin in the world. It is the largest delta in Africa with a subaerial extent of about 75,000 km2 and a sedimentary basin fill of about 9 to 12 km [5]. The geology of the Niger Delta basin has been previously and extensively presented in several key publications [4-10]. The Onshore Niger delta lies between latitudes 4° and 6° N and longitudes 4°30′ and 8°001E (Fig. 1). The boundaries of the onshore portion of the Niger Delta basin are defined by the geology of southern Nigeria and southwestern Cameroon. The basin is bounded in the north by the Benin Flank, which is an east-northeast trending hinge line south of the West African basement massif. Within the north-eastern flank, it is bounded by the outcrops of the Cretaceous sediments of the Abakaliki High and within the east-south-east area, it is bounded by the Calabar flank, which is a hinge line bordering the adjacent Precambrian basement in the southern end. Tectonically, the Niger Delta basin is generally believed to be associated with the stresses that accompanied the separation of the African and South American plates, which resulted in the opening of the South Atlantic.

Lithostratigraphically, the Niger Delta is divided into three pronounced units, which include the Benin Formation mainly coastal plain sands, the Agbada Formation (reservoir sands), and the Akata Formation (source rock) which is made up of the over pressured ductile shales. The stratigraphy of the basin was made more complex by the syn-depositional collapse of the thick assemblage of sediments as the shales of the Akata Formation mobilized under the heavy load of the deltaic Agbada and fluvial Benin Formation deposits as the advanced towards the sea. Three major depositional cycles have been identified within Niger Delta [5,9]. The first two, which involved mainly marine deposition, began with a middle Cretaceous marine incursion and ended in a major Paleocene marine transgression. The second cycle started in the late Paleocene to Eocene time and reflected the progradation of a "true" delta, with an arcuate, wave- and tide-dominated coastline. These sediments range in age from Eocene in the north to Quaternary in the south [9]. Deposits of the last depositional cycle have been divided into a series of six depositional belts often separated by major syn-sedimentary fault zones [9].

### 1.2. Causes of overpressure in the onshore

The causes of overpressure, its distribution, and drilling implications on the Onshore Niger Delta basin have been published by several authors with evidence of secondary mechanisms. Similarly, the shallow Offshore and Onshore areas of the Niger Delta have been proven to have varying clay mineralogy. For instance, the Akata Formation clay mineral assemblage consists of about 35-60% kaolinite, 20-50% smectite, and 10-30% illite while, the Agbada Formation has varying clay mineralogy of about 40-75% kaolinite and 10-35% smectite according to Lambert-Aikhionbare and Shaw [11]. In the young deltaic sedimentary basin, disequilibrium compaction is the active cause of overpressure, but at deeper depths, within the Onshore Niger Delta, secondary mechanisms such as shale unloading can play out. The depth at which shale unloading (including fluid expansion, aqua-thermal,clay diagenesis ) occurs varies across the different depositional belts of the Niger Delta Basin but generally starts from the depth range of 3108.96 to 3352.8m below the mud line which is a corresponding temperature of 93 to 100°C [12-13]. Similarly, Lambert-Aikhionbare and Shaw [11] posited that burial diagenesis have minimal effect on the clay mineralogy of the Agbada and Akata shales at around 12,000 ft (3657.6m) and geothermal temperature of 120°C and confirmed that smectite is present at temperatures of 105-110°C in the Agbada Formation shales. The work of Nwozor, *et al.* [14] and Chukwuma *et al*. [15] validated smectite-illite transformation and shale loading hence, they used Eaton's exponent of 5 and 7 at depth > 3800m below mudline for Coastal and Central Swamp depobelts, respectively, in Onshore Niger Delta.

## 2. Theory and method

The methodology involved in the prediction of pore pressure of shale-rich rocks include the analysis of seismic and well data based on the simple principles that: (1) high pressure is associated with higher than expected porosity; (2) the parameter used to capture porosity is of good quality with high data density; and (3) porosity and rock property coefficients are a function of the Maximum Vertical Effective Stress (MVES). Vertical effective stress is the net stress acting on a rock in the vertical sense, i.e., the force acting downwards due to the weight of the rocks above (the overburden stress) counter-acted by pore fluid pressure. Based on this premise, Terzaghi's and Biot's effective stress law [16-17] has been the foundation for most of the pore pressure estimation techniques over the years. This theory indicates that pore pressure in the formation is a function of overburden stress and effective stress. Therefore, if the overburden stress and vertical effective stress are known, the pore pressure can be determined using the Terzaghi's equation given as:

$$P_P = \frac{(Sv-\sigma_{eff})}{\alpha} \qquad (1)$$

where *Pp* is the pore pressure; $S_v$ is the overburden stress; $\boldsymbol{\sigma_{eff}}$ is the vertical effective stress; and $\alpha$ is the Biot effective stress coefficient always assumed to be 1 or less in most pore pressure studies [13,18-19].

In this study, RokDoc™ software was first used to define the normal compaction trend and overburden model for the studied area based on equations 2 & 3, respectively.

$$V_p(zml) = V_{p(matrix)} - (V_{p(matrix)} - V_{p(top)})e^{-b(zml)} \qquad (2)$$

where $V_{p(top)}$ is the surface velocity with values of 5250 ft/s; $V_{p(matrix)}$ is the matrix or velocity value at the base of the interval defined to be 19830 ft/s for the field; $-b$ is a value that determines the compaction rate of the sediments known as the compaction coefficient with values of 1.21920E-4 in this study; but it is dependent on the compaction state of the rocks.

Similarly, Equation 3 was used to define the overburden gradient.

$$Rho(zml) = Rho_{(matrix)} - (Rho_{(matrix)} - Rho_{(top)})e^{-b(zml)} \tag{3}$$

where $Rho_{(top)}$ represents density value at the surface defined here to be 1.8 g/cc; $Rho_{(matrix)}$ is equal to 2.6 g/cc depth intervals, and; $-b$ equal to 1.00610E-4 represents the compaction coefficient.

But to achieve a rock model that can relate seismic to subsurface pressure, Equation 4 was used on the excel spreadsheet.

$$S_v = 0.95 * Depth + 14.7 \tag{4}$$

where 14.7 psia represents standard atmospheric pressure (i.e. atmospheric pressure taken into account).

No water depths since the wells are from the Onshore Niger Delta field. The unit pounds per square inch absolute (psia) are used to make it clear that the pressure is relative to a vacuum rather than the ambient atmospheric pressure. However, it is a known fact that different mineralogies, porosities, and fluids do change the lithostatic pressure gradient.

Effective stress and sonic velocity relationship are unique in the sense that challenges encountered with the 'normal' compaction trend method in complex geology especially, where depth is used as a geologic substitute that controls pressure distribution can be overcome [20].

Bowers [21] presented a velocity-effective stress relationship (Eq. 5) for effective pressure estimation when disequilibrium compaction is the predominant cause of overpressure.

$$\sigma_{eff} = \left[\frac{V-V_0}{A}\right]^{\frac{1}{B}} \tag{5}$$

where $V$ is the velocity at a given depth; $V_0$ is the surface velocity (normally 5000 ft/s); $\sigma_{eff}$ is the vertical effective stress; and parameter $A$ and $B$ can be obtained from calibrating regional offset velocity versus effective stress data, though the process could be cumbersome especially, where there is paucity of data.

The predominant cause of overpressure in the studied area (Field X) has been proven to be under compaction with the successful use of Eaton's empirical and Equivalent depth methods. However, the goal of this study is to derive the input coefficient for Equations 6:

$$\sigma_{eff} = Ae^{B*V_p} \tag{6}$$

where $V_p$ is seismic, or well velocity, and $A$ & $B$ are the parameters to be determined from the equation of an exponential fit on the shale velocity vs. effective stress crossplot. The crossplotted data points were painstakingly extracted from the shale adjacent to the undrained reservoir pressures in the wells.

The one dimension (1D) shale pressure estimate was based on Eaton's [22] empirical formula (Eq. 7) with Equations 2&3 above as input models.

$$P_P = S_v - (S_v - P_{hydro})\left(\frac{\Delta t_{norm}}{\Delta t_{obs}}\right)^x \tag{7}$$

where $P_p$ is the pore pressure; $P_{hydro}$ is the hydrostatic pressure taken to be 0.433 psi; $\Delta t_{obs}$ is the measured or observed sonic transit time in shale obtained from well logging; $\Delta t_{norm}$ is the sonic transit time in shale at the normal pressure condition obtained from normal trend line (equation 2), and the $x$ exponential constant was taken to be 3 for overpressure caused by disequilibrium compaction. However, in some parts of the Onshore Niger Delta (e.g., Northern Delta depobelt), the exponent can be raised to 5 or 6 for areas where secondary mechanisms are believed to be responsible for overpressure generation [13].

### 2.1. Velocity analysis

Futhermore, semblance displays were used to interpret the interval velocity functions, in both time and depth. Two seismic vintages mainly, isotropic and anisotropic migrated seismic velocities covering the studied area were carefully picked using 100m and 200m grid. The seismic velocity was derived by the analyses of the stacking velocity picks, semblance panel, and common mid-point (CMP) gathers or hyperbolic moveout with offset using Shell™ in-house software. The different stacking velocity analysis represents the first group of techniques aimed at perfecting the seismically driven 3-D image of the subsurface. Generally, the various interval seismic velocity estimations based on conventional stacking data analysis (RMS, CMP, DMO, CRP, CRE velocity analysis, etc.) do not possess oriented kinematical characteristics of the wave field, despite the fact that they are often misused for overpressure prediction. Often times, these velocity vintages do not have the appropriate resolution needed for pore pressure prediction studies.

To ensure the velocities are within the realm of expected rock velocities, the Dix linear relationship was used to obtain the interval velocities ($V_{int}$), and especially, the isotropic seismic $V_{int}$ was calibrated to the check shot data using equation 8.

$$V_{int} = V_0 + K_z \quad (8)$$

where: $V_{int}$ = Interval velocity; $V_0$ is the assumed velocity at near-surface; *K* is velocity gradient in ft/sec/ft or 1/sec and Z, is depth in ft or m.

A key step in the velocity analysis was to use rock physics to constrain the interval velocities so that the velocities are meaningful and without spikes or outliers, which are the features that invalidate any routine use of stacking velocities for pore pressure interpretation. A cross-plot of the well check shot and Vp-sonic log provided the equation of the line that was used to constrain the seismic interval velocities.

## 3. Results interpretation and discussion

The plotted wells revealed that the onset of mild overpressure started at ~10000 ft ss while hard overpressure (>0.6 psi/ft) began at ~12200 ft ss or 3.0 seconds (Fig. 2 track 3).

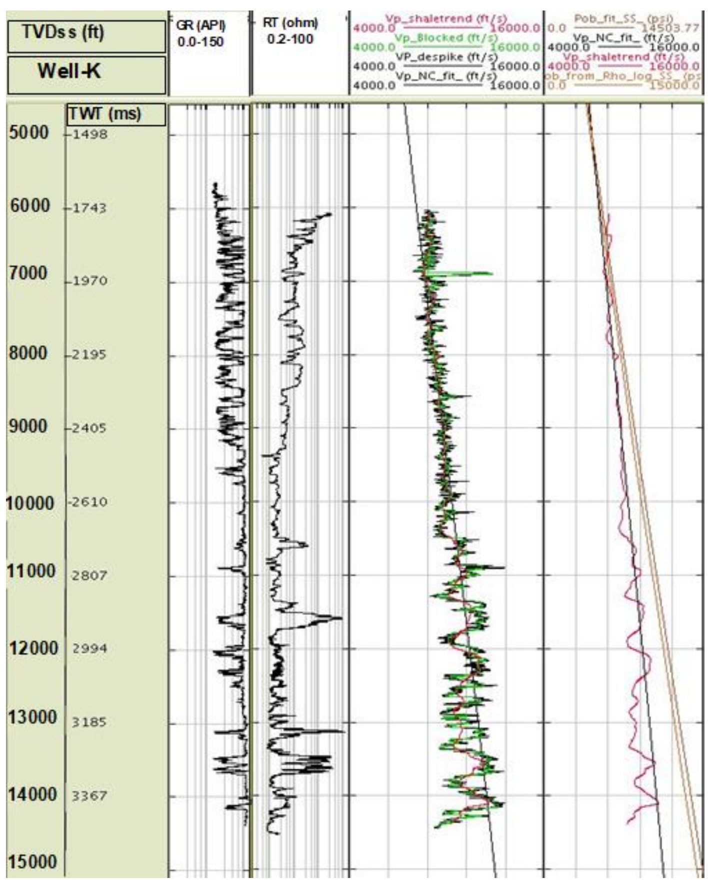


Figure 2. The plot of petrophysical well logs, shale velocity and NCT for well -K

The anomalous increase and decrease in the Vp_shale trend within 10000-12200 ft ss interval could be attributed to local compaction due to the geology of the immediate vicinity. Figure 3 shows the different trends and the coefficients for Eq. 6, which are the effective stress models used for transforming petrophysical measurements (e.g., sonic slowness) to pore pressure in shale, mud, and fine silt beds. The sediment compaction exponential curves were based on interpretation from Well-J (normally pressured) and Well-K (abnormally pressured). The equations of the lines (blue and red) (Fig. 3) are the Vp-VES transforms applied to invert the seismic $V_{int}$ to VES and, with Terzaghi's expression, seismically-derived PP matched the true formation pressure.

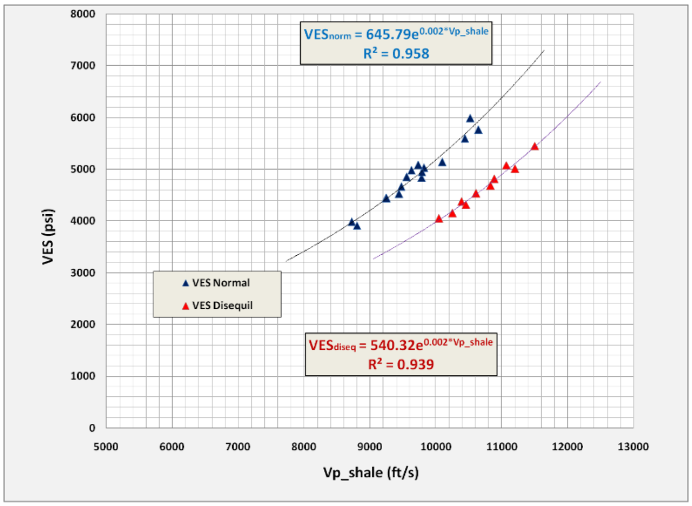


Figure 3. Vertical effective stress (VES) versus shale velocity plot

The challenges of picking multiples, that is, a false impression of overpressure abounds, but, in reality, when assessing seismic velocities using software picking programmes, the seismic reflections are shown as clouds of data. A margin of ± 10% over which a gather will flatten, and seismic velocity can fluctuate over the range of 20% may exist. Where the data is very dense, the reflections are typically the strongest. It is, therefore, easier to pick velocities where reflections are abundant, as demonstrated by the semblance panel showing seismic $V_{int}$ regression and CMP gather in Figures 4 & 5.

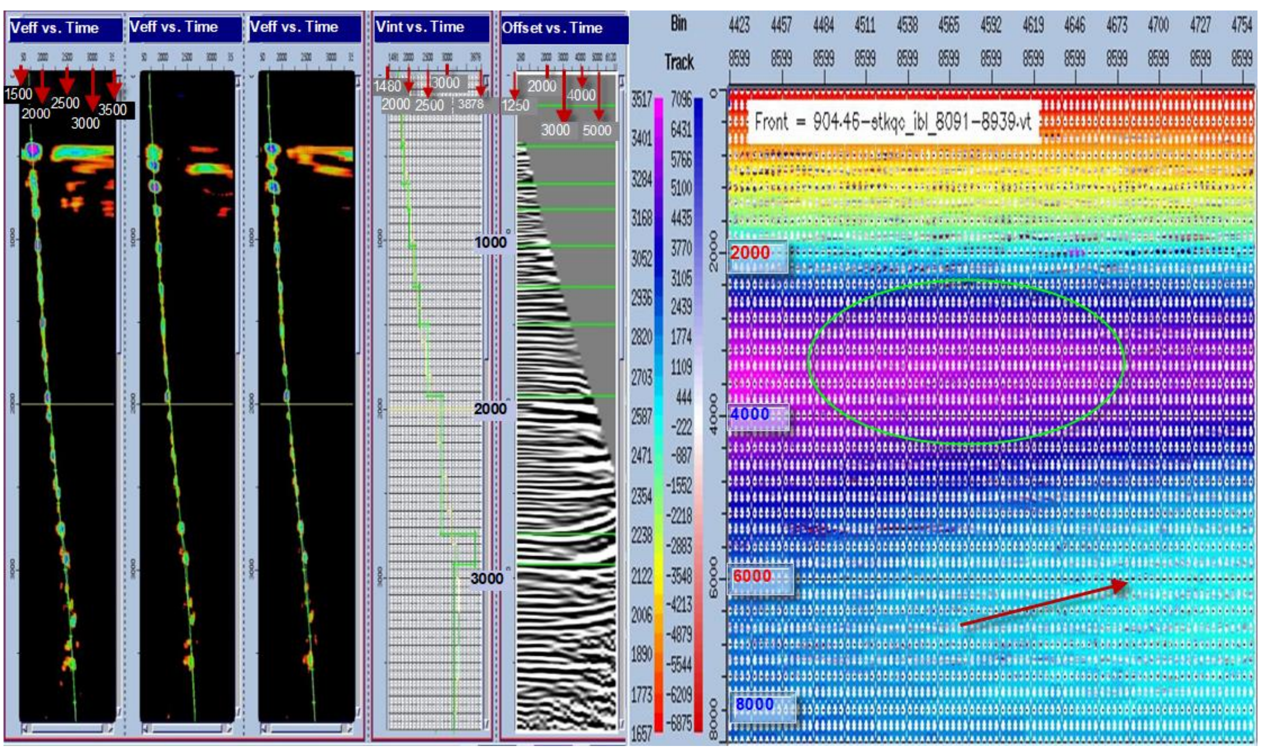


Figure 4. Semblance Panel; Seismic $V_{int}$ regression; CMP Gather and isotropic PSDM velocity field

The comparison of the two seismic velocity models revealed that anisotropic pre-stack depth migrated (PSDM) velocity has better focusing in the stack depth section as indicated by the observed reversal (yellow cluster in the red box) (Fig. 5) around 4400 to 6300 milliseconds. This observed velocity reversal (overpressure signal) imaged at the observed depth was completely missing out, as indicated by the red arrow (Fig. 4). However, both vintages show high resolution at ~2200 to 4200 milliseconds interval, as shown by the oval-shaped region of Figure 4 and the white arrows in Figure 5. Nonetheless, it was more obvious on the anisotropic velocity field seeing that; it responded to any little variations in rock formation properties as it travels through the subsurface as seen below 6.4 seconds (Fig. 5). This is not unconnected to the fact that rock types, porosity, and clay content affect velocity and that; lithology directly affects velocity through matrix density and matrix velocity [23]. It is expected that velocity will increase downward as one goes from the unlithified or unconsolidated sediments and soils at the surface into consolidated bedrock. Similarly, velocity increases as one travel from the vadose or unsaturated zone to the phreatic or saturated zones. These systematic velocity changes can be related to lithology, degree of cementation, increasing hydrostatic pressure, and replacement of air in the pore space by water [23]. Worth noting is that an increase in shale content lowers velocity and porosity has a greater influence on velocity than shaliness. Moreso, observed hard overpressures are associated with intervals with thick shale in the Niger Delta sedimentary basin. As observed here, the velocity models especially, the anisotropic PSDM, proved robust as the signatures of the varying lithology (i.e., the composition of the rock solids) with depth are adequately imaged in time and space. It is proof also that rock-forming minerals have different elastic properties, causing systematic velocity differences between lithologies.

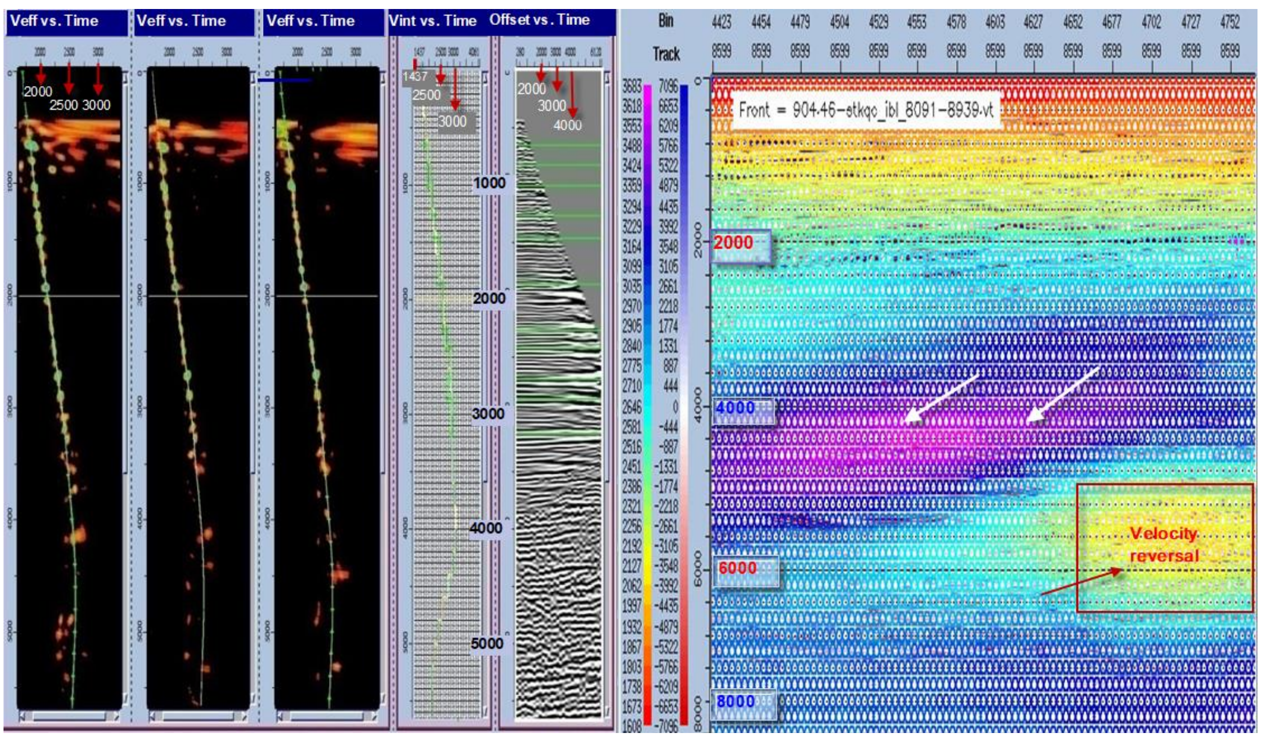


Figure 5. Semblance Panel; Seismic $V_{int}$ regression; CMP Gather and anisotropic PSDM velocity field

The analyses of the adopted picking patterns (100m and 200m) show little or no alteration to the velocity profile seeing a close match of the seismic $V_{int}$ trends in Figure 6. Also, observation shows that isotropic PSDM seismic velocity (green/red trends) picked 100m/200m as shown on the legend to the left was migrated much faster than the true velocity of the subsurface starting at around 2000 milliseconds where the onset of anisotropy began in the field (Fig. 6). Based on that, the deeper structures are expected to be mispositioned in both depth, and lateral location since anisotropy was not accounted for at 2.0 seconds deeper. So, the inset on the left side of Figure 6 showed the calibration of isotropic seismic $V_{int}$ to check shot. The agreement between the check shot (green), seismic interval velocity (gray), $V_oK$ analysis and Fit-specific depth function shows that the resolution of the extracted interval velocity was reasonable, i.e., geologically, significant changes in the velocity field can be observed within the resolution (Fig. 6 inset). The purple/yellow trends picked 100m/200m from the anisotropic seismic volume (Fig. 5) and plotted as $V_{int}$ versus time represented the true vertical subsurface velocity; hence, no further calibration was applied (Fig. 6).

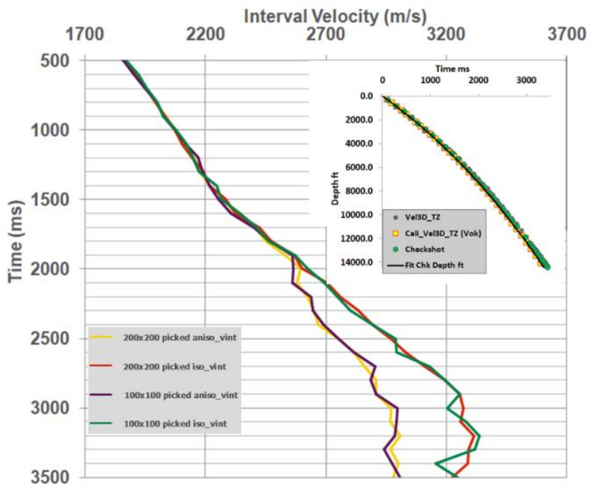


Figure 6. The plot of interval velocity vs. Time; calibration and the different (100m & 200m) picking pattern

The Well-K used here is deviated, and it is a common knowledge that shale anisotropy can cause borehole sonic logs acquired in deviated wells to be significantly faster than those acquired in vertical wells [24]. Therefore, the sonic log is not expected to offer a good match except if corrected for anisotropy.

Peaks and reversals are the most diagnostic features for determining the degree of anisotropy, and in theory, the interval velocity field (in-depth) from an anisotropic model represents the true vertical velocity of the well and is closer to sonic (true vertical) velocity as well as check shot interval velocities. In previous studies, the possible presence of seismic velocity anisotropy was detected by plotting seismic velocity data with borehole sonic log and check shot data inverted to sonic velocities [3,25]. The trend of the seismic velocity plot with respect to the borehole sonic was then used to detect the presence of anisotropy. But recently and as demonstrated here, the sensitivity of seismic velocities to pore pressure has been enhanced due to improved seismic resolution resulting from long offset, wide azimuth data. Seismic imaging that is very accurate in-depth and space can be produced [26] with a robust seismic velocity modelling.

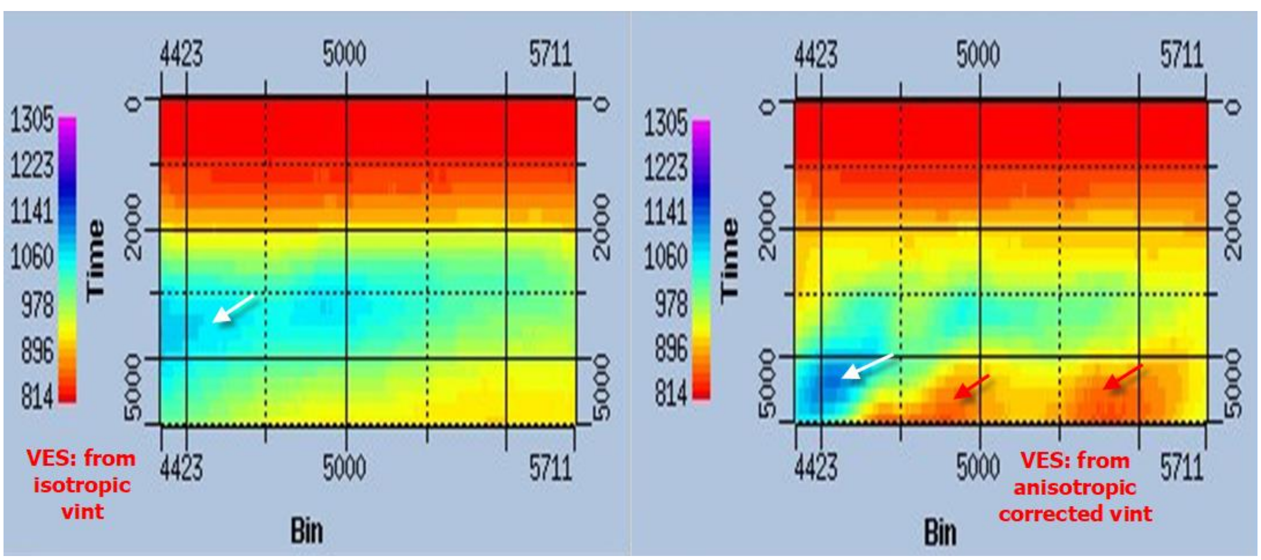


Figure 7.VES cube obtained using the normally pressured curve equation

The improved resolution, as shown by the different seismic vintages, was reflected in the transformed VES cubes (Figs. 7 & 8) using the Vp-VES derived here. The arrows are indicative of the benefits and improvements gained by taking anisotropy into account (Figs. 7 & 8). Pore pressure increment is numerically equal to the effective stress decrease, resulting to increase in the stress field as depth increases. Thus, the white arrows in Figure 8 are a pointer to a zone of reduced pore pressure in the steeply dipping high VES zone (magenta). This is reflective of the fact that overpressure is coupled with stress, and an increase in pore pressure will reduce VES, and so, the zone of high VES was reflective of pore pressure decrease (i.e., porosity reversal). Again, to the right of Figures 7 & 8 (below 5.0 seconds) are two red arrows indicating a lateral reversal of VES. These changes in VES could be attributed to load distribution whose direct implications are changes in rock volume, shape, and strength.

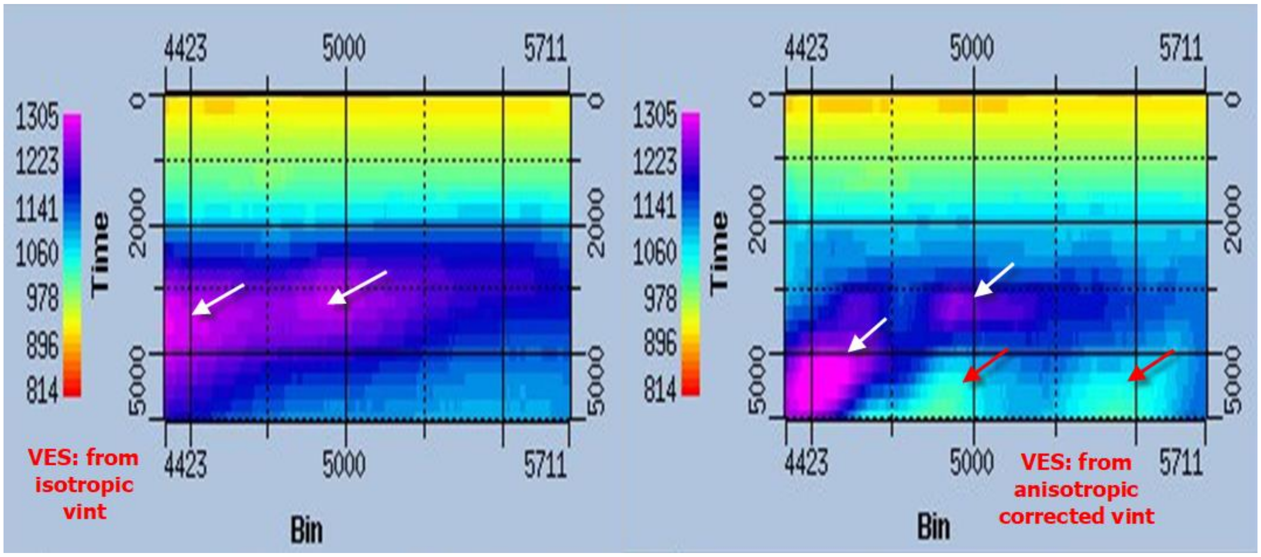


Figure 8. VES cube obtained for the overpressured zone using the disequilibrium equation

The purple data points in Figure 9, are seismically-derived PP from the anisotropic seismic $V_{int}$ when the Vp-VES normal compaction transform was applied. The result was somewhat correlated with the reservoir pressures (blue RFT points) and shale pressure (red data points) at ~14300 ft ss (4358.64m) with an allowable pressure difference of 474 psi. Although, at the shallow hydrostatic interval, the observed pressure differential was around 11300 ft ss (3444.24m) shallower in excess of 1234 psi (Fig. 9).

Likewise, the green data points are the seismically-derived PP when the disequilibrium compaction Vp-VES model was applied on anisotropic seismic $V_{int}$ while the black closed circle data points were from the calibrated isotropic seismic $V_{int}$. Both were seen to match the reservoir pressures (RFT points in blue) pretty well (Fig. 9) except, at 11300 ft ss shallower where observed pressure differential was as high as 1899 psi. Similarly, the open circled data points are seismically derived PP inverted from the isotropic velocity field using the normal compaction Vp-VES model, and the result also matched the reservoir pressures within the hydrostatic or normally pressured intervals (i.e., at ~11620 ft ss shallower) (Figs. 9 & 10). The blue RFTs points that fell far below the hydrostatic gradient could mean drained sands interval in Well-K but, such pressure depletion was not observed in Well-J. The hydrostatic gradient of 0.433 psi/ft was defined, and in practice, the open circle data points around 6900 – 77800 ft ss (Figs. 9 & 10) were meant to be clipped to the hydrostatic gradient.

From the foregoing, a single normal compaction Vp-VES model (such that gave the purple data points in Figure 9) could suffice in inverting for seismic PP, from anisotropically PSDM velocity since wells are generally drilled overbalanced, and the uncertainty at shallow and deeper levels are known. Overpressures in the field nearly reached 0.7 psi/ft at depths greater than 14,500 ft ss, and the seismically-derived PP from both vintages were observed to match the reservoir pressures with little or no uncertainty (black close circle and green data points) at depth in Figure. 10.

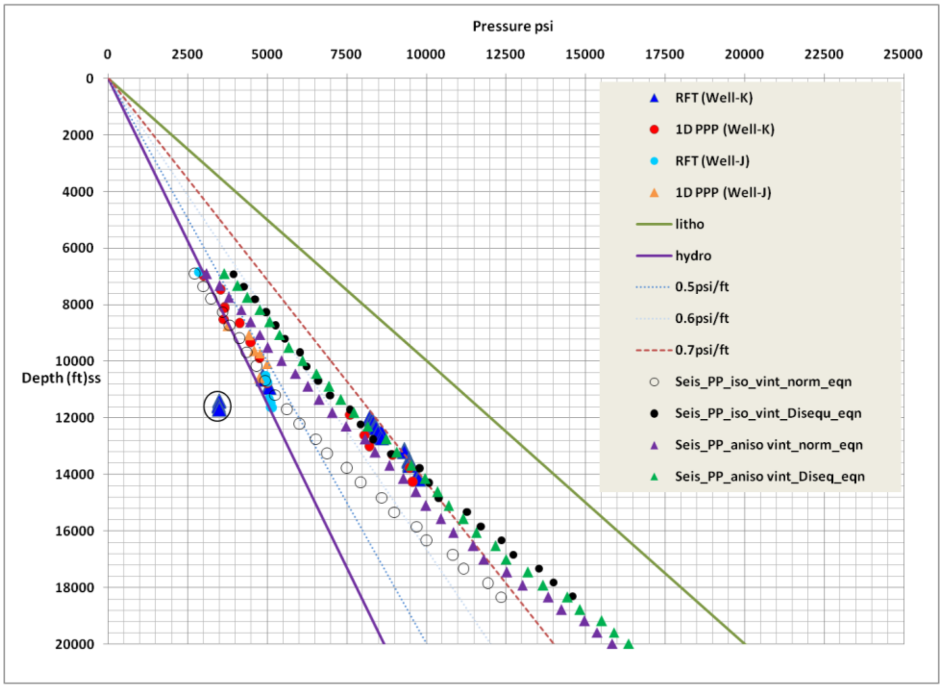


Figure 9. Comparison of the normal and disequilibrium compaction Vp-VES models used in transforming seismic $V_{int}$ into pore pressure.

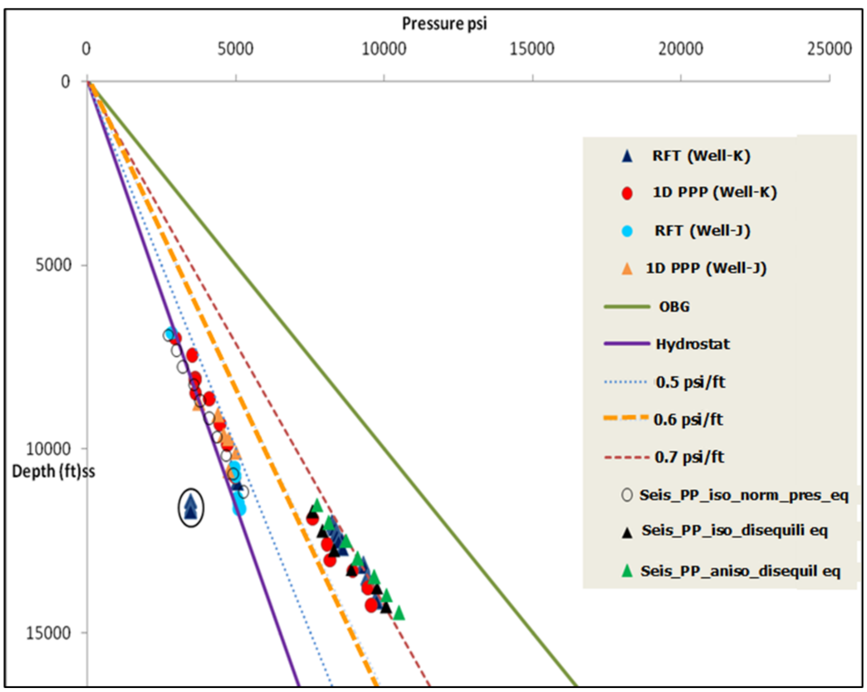


Figure 10. Pore pressure derived from seismic velocities: anisotropic (green data) &isotropic (black data points) and compared with directly measured pressures (RFT) and 1D PP estimate (red & orange data points) in the wells

This makes the disequilibrium compaction Vp-VES model more useful as wells are currently drilled beyond 12000 to 16000 ft ss in Onshore Niger Delta. Therefore, with isotropically PSDM velocity field and adequate calibration, the derived disequilibrium compaction Vp-VES exponential curve can image subsurface pressure beyond ~3.0 s where hard overpressures are mostly encountered in Niger Delta, and this applies to anisotropically PSDM velocity too. The hydrostatic (normally pressured) or mildly overpressured intervals (i.e., zones having pressure gradient < 0.5 psi/ft) are less of interest so, with the uncertainties provided here the normal compaction Vp-VES regression can be a quick and simple model in transforming anisotropically migrated seismic velocity to pore pressure cube from shallow to deeper intervals.

## 4. Summary, conclusion, and recommendation

The analyses in this study have shown the closeness of the seismic pore pressure to the predicted shale pressures, which is a proof that the derived Vp-VES coefficients can provide a quick estimate of seismic pore pressure as it links the observed data to predicted pressures in the studied area. It further established that sonic velocities could be estimated from VES and lithology dependent constants representing the properties of the rock with zero porosity since they are a function of the porosity and rock property coefficients. Seismically-derived pore pressure can be less accurate especially at depth in the presence of errors in the velocity field and is usually not fit for optimum well planning hence; this work has proven the fidelity of the (isotropic and anisotropic) PSDM velocity models as they offered superior imaging in the vertical and lateral positioning at larger times and are depth consistent down the wells. The geological information in the examined area was made more pronounced by the isotropic and anisotropic PSDM velocity models thereby making the seismic velocities fields suitable for any quantitative pore pressure. Hence, the benefit of incorporating well data in the velocity-depth model is emphasized. Worthy of mention is that, when lateral velocity variations and dipping structures exist, pressure prediction from the Dix equation $V_{int}$ can be in error, and can become unstable when the stacking velocity decreases [2,27]. These problems can occur in over-pressured areas but, with skillful velocity picking and the use of depth migrated velocity, more accurate lateral interval velocities in the depth domain can be made possible. The current practices of 100m or 200m velocity picking or spacing provided adequate resolution and resulted in optimal seismic pore pressure estimation.

The anisotropic velocity field therefore needs minimal or no further calibration even at deeper intervals, even in sedimentary basins like the Niger Delta where shales seem inhomogeneous and are up to 75% in composition [24]. In view of this therefore, accounting for anisotropy in the velocity model and on long offset data will significantly reduce uncertainties in subsurface pressure interpretation especially now that deeper wells of 16000 ft ss and beyond are been drilled. In addition, at ~3.0 seconds (~12200 375 ft ss) where the onset of hard overpressure began, the disequilibrium compaction Vp-VES model can be adapted for nearby prospects, provided care is taken to condition the seismic velocities and ensure that robust rock physics model relations are extracted from well data. The derived coefficients can be inputted into any software with the user-defined calculator, thereby saving time and overcoming the challenges that paucity of data may pose in such offset areas. However, detailed knowledge of the local geology, depth to overpressure and shale unloading in such areas must be inferred from offset wells as a guide to selecting the appropriate model for optimal seismic pore pressure prediction.

***Acknowledgment***

*The authors wish to thank the University Liaison Unit of Shell Petroleum Development Company Limited for providing the data sets, hardware as well as the software used in this research work. We also acknowledge with thanks the contributions of many of our colleagues at the Geo-solutions department for their input.*

**References**

[1] Mukerji T, Dutta N, Prasad M, and Dvorkin J. Seismic detection and estimation: Part I: the Rock Physics Basis, CSEG Recorder, September 2002.
[2] Dutta NC. Deepwater geohazard prediction using prestack inversion of large offset P-wave data and rock model. The Leading Edge, 2002; 21(2): 193-198.
[3] Opara AI, and Onuoha KM. Pre-drill pore pressure prediction from 3-D seismic data in parts of the Onshore Niger Delta basin. 33rd Annual SPE International Technical Conference and Exhibition in Abuja, Nigeria, August 3-5, 2009, SPE 128354; 12.

[4] Merki PI. Structural Geology of Cenozoic Niger Delta. In First African Regional Geological Conference 1970; Proceedings, Ibadan University Press 1972, pp. 251-266.
[5] Short KC, and Stauble AJ. Outline Geology of the Niger Delta. AAPG Bull., 1967; 51; 761-779.
[6] Evamy BD, Harembourne J, Kamerling P, Knaap WA, Molley FA, Rowlands PH. Hydrocarbon habitat of the Tertiary Niger Delta. AAPG Bull., 1978; 62(1): 1-39.
Opara AI, Onuha KM, Anowai C, Onu NN, Mbah R. Geopressure and Trap Integrity Predictions from 3-D Seismic Data: Case Study of the Greater Ughelli Depobelt, Niger Delta. Oil & Gas Science and Technology - Revue de l IFP, 2013; 68(2): 383-396.
[7] Weber KJ. Hydrocarbon distribution patterns in Nigerian growth fault structures controlled by structural style and stratigraphy. Journal of Petroleum Science and Engineering,1987; 1: 91-104.
[8] Weber KJ. 1971. Sedimentological aspects of oil fields in the Niger Delta. Geologie en Mijnbouw, 1971; 50: 559–576.
[9] Doust H, Omatsola E. Niger Delta. In Divergent/passive Margin basins. Edwards JD, Santogrossi PA. (eds), AAPG Memoir, 1990; 45: 239-248.
[10] Weber KJ, Daukoru EM. Petroleum geology of the Niger Delta. World Petroleum Congress Proceedings, 1975; 2: 209-221.
[11] Lambert-Aikhionbare D, and Shaw H. Significance of Clays in the Petroleum Geology of the Niger Delta: Clay Minerals, 1982; 17: 91-103.
[12] Opara AI, Onuoha KM, Igbokwe S, Anowai C, and Onu NN. A New Velocity Effective Stress Model for Estimating Overpressure Mechanisms besides Compaction Disequilibrium; NAPE Bulletin, 2008; 20(2): 17-23.
[13] Asedegbega JE, Oladunjoye MA, and Nwozor KK. A method to reduce the uncertainty of pressure prediction in HPHT prospects: a case study of Onshore Niger Delta depobelt, Nigeria. Petrol Explor Prod Technol., 2017; 1-6
[14] Nwozor K, Omudu M, Ozumba B, Egbuachor C, and Odoh B. A Relationship Between Diagenetic Clay Minerals and Pore Pressures in an Onshore Niger Delta Field. Petroleum Technology Development Journal, 2012; 2: 18.
[15] Chukwuma M, Brunel C, Cornu T, and Carre G. Overcoming Pressure Limitations in Niger Delta Basin: digging Deep into New Frontier on Block-X. Journal of Geology and Geosciences, 2013; 2(1): 1000112.
[16] Biot MA. General theory of three-dimensional consolidation. J Appl. Phys., 1941; 12: 55–164
[17] Terzaghi K, and Peck RB. Soil mechanics in engineering practice: New York 1948, J Wiley. 566.
[18] Zhang J. Pore pressure prediction from well logs: Methods, modifications, and new approaches. Article Earth-Science Reviews, 2011; 108(1-2): 1-15.
[19] Azadpour M, Manaman NS, Kadkhodaie-Ilkhchi A, and Sedghipour M. Pore pressure prediction and modeling using well-logging data in one of the gas fields in south of Iran. J Petrol SciEng., 2015; 128:15–23.
[20] Dutta NC, and Khazanehdari J. Estimation of formation fluid pressure using high-resolution velocity from inversion of seismic data and rockphysics model based on compaction and burial diagenesis of shales. The leading edge, 2006; 25: 1529-1539.
[21] Bowers GL. Determining an appropriate pore-pressure estimation strategy. Offshore Technology Conference (OTC 13042): Houston 2001, TX. 2-14.
[22] Eaton BA. The Equation for Geopressure Prediction from Well Logs. 50th Annual Fall Meeting of the Society of Petroleum Engineers of AIME 1975: Dallas Texas, SPE paper #5544.
[23] Butler DK. An Introduction to Rock Physics for Near-Surface Geophysics. SEG, 2005; 13: 31-70.
[24] Brian EH, John MH, and Donald WI. Anisotropy correction for deviated-well sonic logs: Application to seismic well tie. SEG, 2003; 68(2): 464-471.
[26] Ehirim CN, Ebeniro JO, and Ogagarue DO. Velocity anisotropy in the Niger Delta Basin: A case study of prestack time imaging with isotropic and anisotropic velocity models. Archives of Physics Research, 2010; 1(2): 50-57.
[27] Chopra S, and Huffman A. Velocity determination for pore pressure prediction. Recorder. 2006; 31(04).
[28] Dix CH. Seismic velocities from surface measurements. Geophysics, 1955; 20: 66-68.


*To whom correspondence should be addressed: Dr. A. I. Opara, Department of Geology, Federal University of Technology, PMB 1526, Owerri, Nigeria, E-mail: oparazanda2001@yahoo.com*